JOURNAL OF MATERIALS SCIENCE **34** (1999) 2837–2842

Microstructure and thermal shock resistance of Al_2O_3 fiber/ZrO_2 and SiC fiber/ZrO_2 composites fabricated by hot pressing

K. PARK
Department of Materials Science and Engineering, Chung-Ju National University, Chungju 380-702, Korea

T. VASILOS
Department of Chemical and Nuclear Engineering, University of Massachusetts, Lowell, MA 01854, USA

Al_2O_3 chopped fiber/ZrO_2 and SiC continuous fiber/ZrO_2 composites were fabricated by hot pressing at 1550 °C and 15 MPa in vacuum. The mechanical properties of thermally shocked composites were measured at room temperature by four-point bending. The addition of Al_2O_3 fibers into ZrO_2 matrix degraded the fracture strength, but improved significantly the thermal shock resistance. In addition, the mechanical properties of SiC fiber/ZrO_2 composites were much lower than those of monolithic ZrO_2 because of the presence of microcracks on the surface. The SiC fiber/ZrO_2 composites showed an excellent thermal shock resistance. © *1999 Kluwer Academic Publishers*

1. Introduction

Zirconia (ZrO_2) has received considerable attention primarily because of its enhanced tensile strength and fracture strength, good wear resistance, and low friction coefficient, compared with other technologically important ceramics. However, ZrO_2 is brittle so that it fails in a brittle fashion with very little deformation to failure. This can be a major problem when it is utilized in weight-bearing areas of the structural applications. The incorporation of reinforcements into ceramics is a potential strategy to improve the mechanical properties [1–3]. The thermal stress of ZrO_2 based composites is generated at the interface between the fiber and matrix due to the difference in the thermal expansion coefficients of the two components, when the composites are subjected to any temperature change, i.e., during cooling from the processing temperature to room temperature or during service. The nature and magnitude of thermal stress remaining at the end of processing or services of the composites are of great importance.

The thermal stress in fiber-reinforced composites has significant effects on the interface sliding stress, matrix cracking stress [4], and ultimate strength [5], and also has been analyzed by a number of researchers [6–9]. It is necessary that ZrO_2 possess good thermal shock resistance for high-temperature applications. Many researchers have studied the thermal shock resistance of Al_2O_3 based composites [10–15], but only a few attempts have been made on the thermal shock resistance of ZrO_2 [16–18]. In this work, we attempted to improve the thermal shock resistance by the incorporation of SiC or Al_2O_3 fibers into ZrO_2 matrix. The SiC fiber/ZrO_2 and Al_2O_3 fiber/ZrO_2 composites were fabricated by hot pressing at 1550 °C and 15 MPa in vacuum.

2. Experimental

The materials used in this study were (1) yttria (5.35 wt %)-doped zirconia powders with an average particle size of 0.43 μm (HYS-3.0; Daichi Kigenso Kagaku Co., Japan), (2) continuous silicon carbide fibers (SCS-6^{TM} and SCS-9^{TM}; Textron Specialty Materials, Lowell, MA, USA), and (3) alumina (α-Al_2O_3) chopped fibers with a length of 40–120 μm (ALMAX; Mitsui Mining Co., New York, NY, USA). The detailed information on the alumina and silicon carbide fibers used is shown in Table I [19–26]. For the fabrication of Al_2O_3 fiber (20 and 30 vol %)/ZrO_2 composites, Al_2O_3 fiber agglomerates were blended with ethanol in a blender. The ZrO_2 powders were then added into the blender and mixed with the fibers to produce a uniform mixture. Also, for the fabrication of SiC fiber (2 vol % SCS-6^{TM} and 2 vol % SCS-9^{TM})/ZrO_2 composites, SiC fibers were spooled off unidirectionally to form a fiber mat with a linear density of 40 fibers/mm. The ZrO_2 powders aligned with SiC fiber mats were loaded into a graphite die in the hot-pressing furnace. The densification of the two composites was achieved by applying temperature and pressure simultaneously in vacuum. It was held at 1550 °C and 15 MPa for 30 minutes before cooling. The Al_2O_3 chopped fibers exhibited a slightly preferred orientation in planes parallel to the pressing direction and were randomly oriented in a plane

TABLE I Properties of the alumina and silicon carbide fibers used [19–26]

	Al_2O_3 fiber	SCS-6™ SiC fiber	SCS-9™ SiC fiber
Diameter (μm)	10	140	79
Density(g/cm^3)	3.6	3.0	2.8
Tensile strength (MPa)	1800	3500	3450
Elastic modules (GPa)	324	430	307
Coefficient of thermal expansion ($\times 10^{-6}$/°C)	8.8	5.2–6.5[a] 2.6–4.0[b]	4.3

[a]Axial thermal expansion coefficient.
[b]Radial thermal expansion coefficient.

perpendicular to the pressing direction. As a comparison, monolithic ZrO_2 was also hot-pressed in the same manner without fibers.

The microstructural characterization was performed by transmission electron microscopy (TEM) and scanning electron microscopy (SEM). To evaluate the thermal shock resistance of the composites and monolithic ZrO_2, they were heated at a selected temperature (140–460 °C) in furnace for 50 minutes, and then quenched into water at 25 °C. The heating temperature was selected on the basis of the estimated temperature (452 °C) required for the development of a crack in monolithic ZrO_2. The mechanical properties of as-fabricated and thermally shocked composites were measured at room temperature by four-point bending in accordance with ASTM standards D790 [27]. The bending tests were performed using an Instron universal testing machine, and load/deflection data were recorded at a crosshead speed of 0.5 mm/min. The support span was 40 mm and the load span was one half of the support span. Three specimens were tested for each thermal shock condition. For the bending tests, the composites and monolithic ZrO_2 were diamond-machined into rectangular bars ($3 \times 4 \times 55$ mm). The fibers in the SiC fiber/ZrO_2 composites were parallel to the longitudinal direction and the direction of load application was perpendicular to the fiber laminae. The tensile surfaces of the composites were perpendicular to the pressing direction so that both the direction of crack propagation and the crack plane were parallel to the hot-pressing direction. The surfaces of test bars were polished with 6 μm diamond polishing compound to produce a mirror finish.

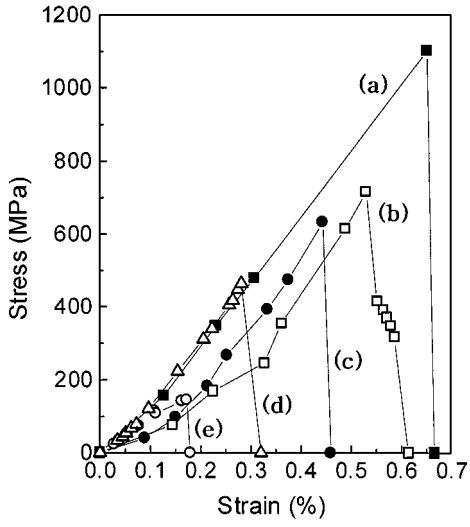

Figure 1 Mechanical properties of as-fabricated (a) monolithic ZrO_2, (b) 20 vol % Al_2O_3 fiber/ZrO_2 composite, (c) 30 vol % Al_2O_3 fiber/ZrO_2 composite, (d) SCS-9™ SiC fiber/ZrO_2 composite, and (e) SCS-6™ SiC fiber/ZrO_2 composite.

3. Results and discussion

3.1. As-fabricated Al_2O_3 fiber/ZrO_2 and SiC fiber/ZrO_2 composites

The mechanical properties of as-fabricated monolithic ZrO_2, Al_2O_3/ZrO_2 composites, and SiC/ZrO_2 composites are shown in Fig. 1. The monolithic ZrO_2 shows a linear elastic loading up to a brittle fracture. The fracture strength and strain to failure of monolithic ZrO_2 are 1112 MPa and 0.67%, respectively. The addition of Al_2O_3 fibers into ZrO_2 matrix degraded the fracture

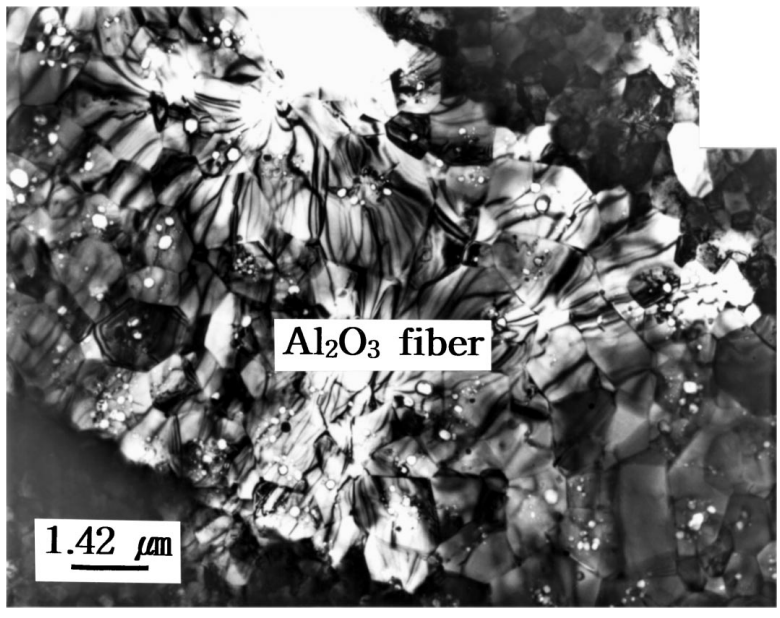

Figure 2 TEM bright field image of Al_2O_3 (20 vol %) fiber/ZrO_2 composite. Note a strong interfacial bond between the matrix and Al_2O_3 fiber.

strength and strain to failure. This is mainly due to the high density of residual pores within the fiber [28] as well as the thermal stress present in the composites. The residual pores were formed during fiber fabrication not during composite fabrication. The pores act as stress concentrators and cracks can be initiated at the pores within the fibers. To improve the mechanical properties, it would be necessary to use pore-free single or polycrystalline alumina fibers.

The thermal stress results from the difference in the thermal expansion coefficients of the fiber and matrix. The thermal expansion coefficients of ZrO_2 and Al_2O_3 have been reported to be $10 \times 10^{-6}/^{\circ}C$ and $8.8 \times 10^{-6}/^{\circ}C$, respectively [19]. Since the thermal expansion coefficient of Al_2O_3 fibers is lower than that of the matrix, upon cooling the matrix grips the fibers. This gives rise to an increase in the strength of interfacial bond, increasing the tendency toward brittleness in the composite. Cracks initiated in the matrix can propagate through the fibers without deflection around the fibers. In addition, although the thermal stress present in the composites is not sufficient to develop microcracks, it superimposes on the applied stress during bending, leading to a decrease in the flexural strength.

It is also important to note that the addition of SiC fibers led to a significant decrease in the fracture strength and strain to failure. This is due to the formation of microcracks in the matrix normal to the filament

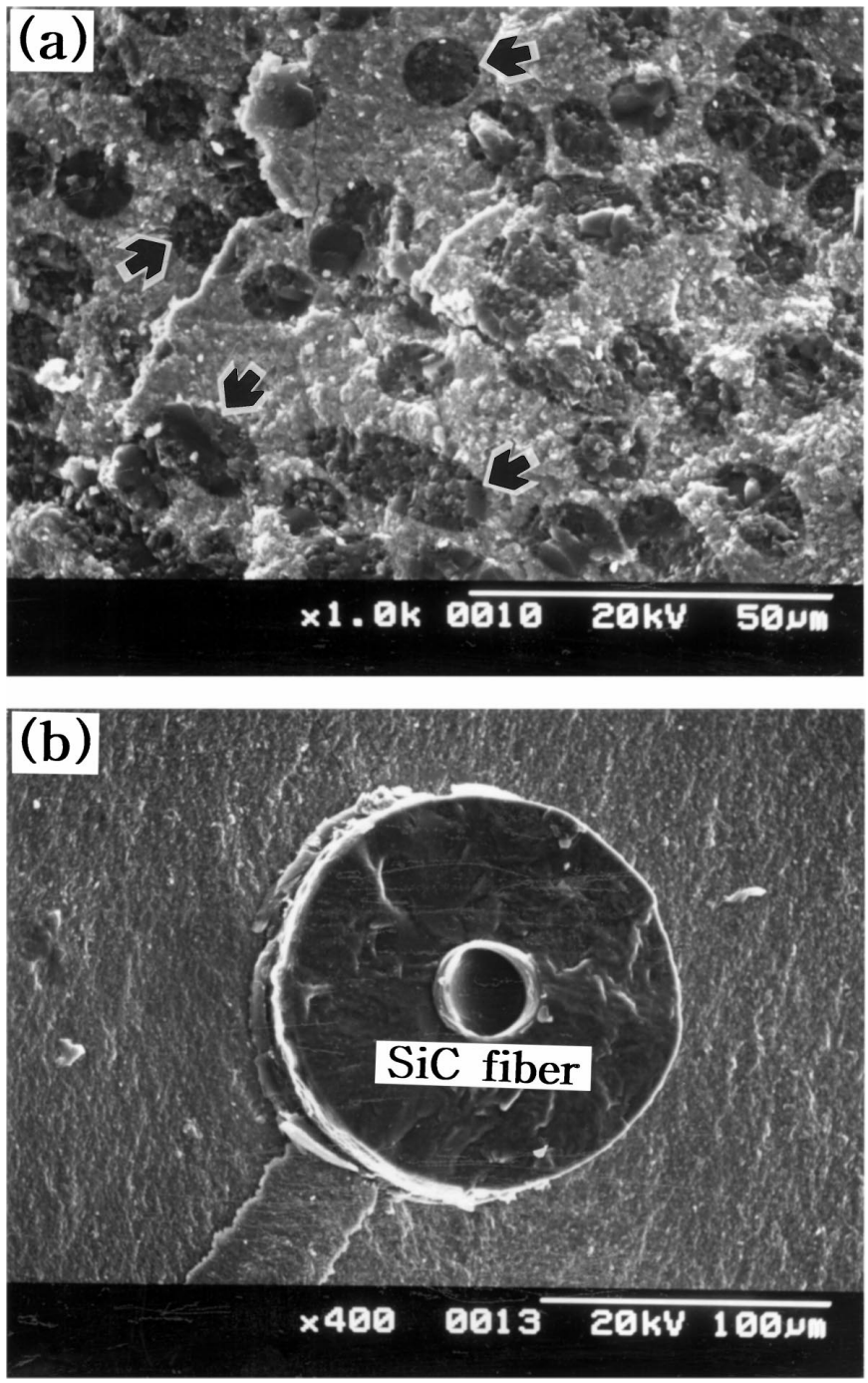

Figure 3 SEM micrographs of fractured surface for as-fabricated (a) Al_2O_3 (30 vol %) fiber/ZrO_2 composite and (b) SCS-6^{TM} SiC fiber/ZrO_2 composite. Some of Al_2O_3 fibers in ZrO_2 matrix are marked by arrows in (a).

axis which could result from the mismatch in thermal expansion behavior between the fiber and matrix. The thermal stress developed by the addition of SiC fibers is larger than that by the addition of Al_2O_3 fibers because of the higher mismatch in thermal expansion coefficient between the matrix and SiC than that between the matrix and Al_2O_3. The thermal expansion coefficients of SCS-6^{TM} and SCS-9^{TM} SiC fibers are given in Table I.

A TEM bright field image showing many residual pores within the fiber and strong interfacial bonding for the Al_2O_3 fiber (20 vol %)/ZrO_2 composite is shown in Fig. 2. In Fig. 2, the interface between the fiber and matrix seems to be strong and sharp, indicating no chemical reaction between the two components. The matrix had equiaxed fine grains because of relatively low temperature (1550 °C) and short time (30 minutes) of hot processing. The microstructure of the ZrO_2 matrix was found to consist of tetragonal precipitates ($a = 0.508$ nm and $c = 0.519$ nm) dispersed in a cubic matrix ($a = 0.513$ nm) [28]. Due to the strong interfacial bonding, a fiber debonding and pullout, required for enhanced toughness, were rarely observed on the fractured surfaces of the composites (Fig. 3).

3.2. Thermally shocked Al_2O_3 fiber/ZrO_2 and SiC fiber/ZrO_2 composites

The monolithic ZrO_2 resulted in a significant reduction in fracture strength and failure strain after thermal shock treatment because of the thermal stress within the material caused by a sudden temperature decrease. As an example, the mechanical properties of the monolithic ZrO_2 thermally shocked from 500 to 25 °C are shown in Fig. 4. The microcracks were found on the surface of the monolithic ZrO_2, resulting in a significant decrease in the mechanical properties. The thermal stress σ on the surface induced by the thermal shock can be calcualted by the following equation [29]:

$$\sigma = \frac{\alpha E}{1 - \nu} \Delta T \quad (1)$$

where α is the thermal expansion coefficient, E is the elastic modulus, ν is the Poisson's ratio, and ΔT is the temperature difference. The thermal stress of the monolithic ZrO_2 thermally shocked from 500 to 25 °C is estimated to be 1242 MPa. This thermal stress is above the fracture stress (~1112 MPa), so that the thermally shocked monolithic ZrO_2 formed cracks under this thermal shock condition. Also, the heating temperature required for a crack formation would be estimated when the thermal stress developed exceeds the fracture stress. The heating temperature for a crack formation estimated from Equation 1 is 452 °C.

On the other hand, the addition of Al_2O_3 fibers into ZrO_2 matrix improved significantly the thermal shock resistance. Fig. 5a and b show the mechanical properties of the Al_2O_3 (20 vol %) fiber/ZrO_2 composite thermally shocked from 425 to 25 °C and of the Al_2O_3 (30 vol %) fiber/ZrO_2 composite thermally shocked from 300 to 25 °C, respectively. It is shown that the 20 and 30 vol % Al_2O_3 fibers/ZrO_2 composites have retained ~46 and ~92% of their unshocked fracture strengths, respectively, after thermal shock treatment. It is likely that during the thermal shock process, the 30 vol % Al_2O_3 fiber/ZrO_2 composite did not form matrix microcracks, but the 20 vol % Al_2O_3 fiber/ZrO_2 composite formed matrix microcracks. The matrix

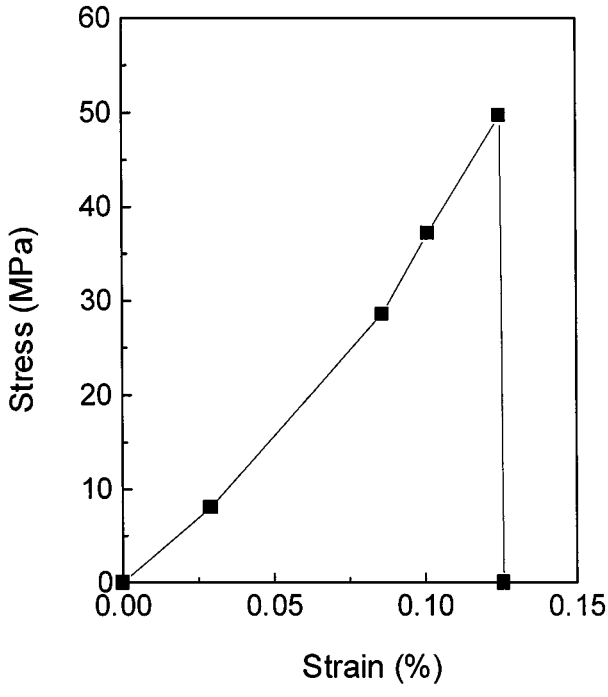

Figure 4 Mechanical properties of the monolithic ZrO_2 thermally shocked from 500 to 25 °C.

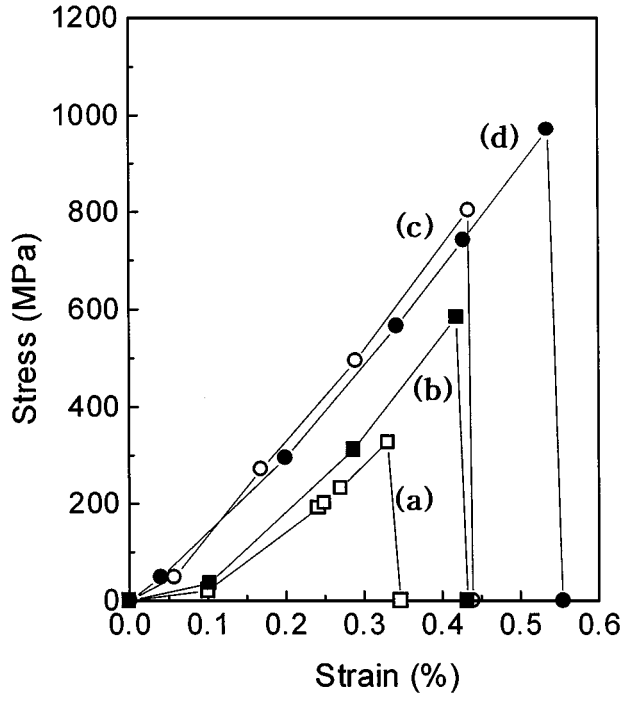

Figure 5 Mechanical properties of the (a) Al_2O_3 (20 vol %) fiber/ZrO_2 composite thermally shocked from 425 to 25 °C, (b) Al_2O_3 (30 vol %) fiber/ZrO_2 composite thermally shocked from 300 to 25 °C, (c) SCS-9^{TM} SiC fiber/ZrO_2 composite thermally shocked from 225 to 25 °C, and (d) SCS-6^{TM} SiC fiber/ZrO_2 composite thermally shocked from 170 to 25 °C.

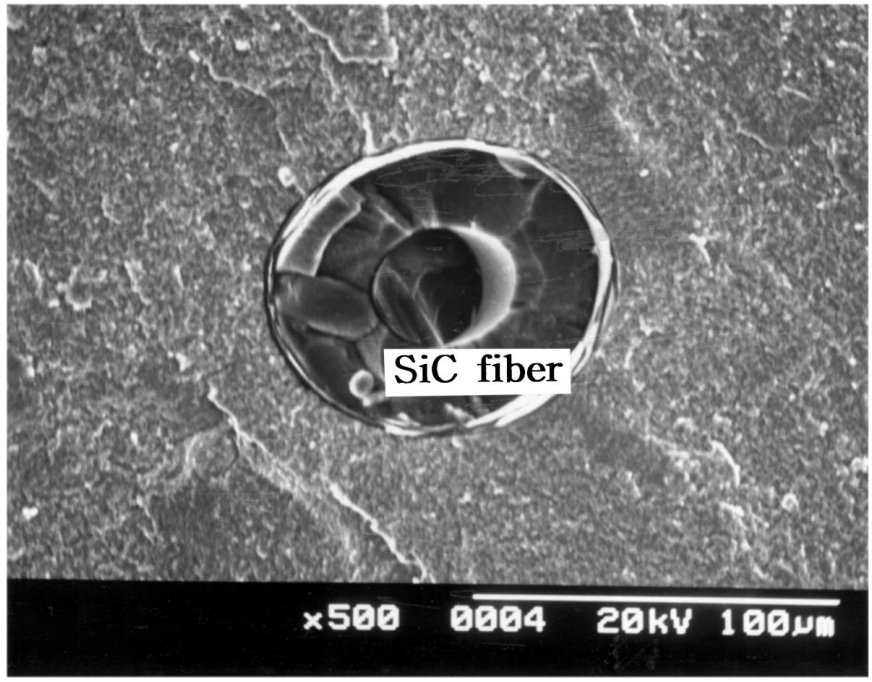

Figure 6 SEM micrograph of fractured surface for the SCS-9^{TM} SiC fiber/ZrO_2 composite thermally shocked from 225 to 25 °C.

microcracks interact with the Al_2O_3 fibers and thus lead to a crack pinning or bridging. The crack interaction contributes to an increase in the thermal shock resistance. In addition, the thermal stress in the composites developed during composite fabrication could be relaxed during thermal shock process. Therefore, the thermal shock resistance of the Al_2O_3 fiber/ZrO_2 composites was enhanced.

In particular, the fracture strength and failure strain of SiC fibers-reinforced ZrO_2 composites were greatly improved after thermal shock process. Fig. 5c and d show the mechanical properties of the SCS-9^{TM} SiC fiber/ZrO_2 composite thermally shocked from 225 to 25 °C and of the SCS-6^{TM} SiC fiber/ZrO_2 composite thermally shocked from 170 to 25 °C, respectively. The mechanical properties of the thermally shocked SiC fibers/ZrO_2 composites were superior to those of as-fabricated ones. As an example, the fracture strength and failure strain of as-fabricated SCS-9^{TM} SiC fiber/ZrO_2 composite are 463 MPa and 0.32%, respectively, while those of the SCS-9^{TM} SiC fiber/ZrO_2 composite thermally shocked from 225 to 25 °C are 803 MPa and 0.44%, respectively. This represents that the fracture strength of SCS-9^{TM} SiC fiber/ZrO_2 composite, after thermal shock quench from 225 to 25 °C, is ∼73% higher than that of the unshocked composite. This improvement seems to be due to the closure of matrix microcracks, which were formed during composite fabrication, due to the tetragonal-to-monoclinic phase transformation in the matrix [30, 31]. The transformation is induced by the external stress associated with the propagation of microcracks which is caused by the thermal shock treatment and causes a volume expansion (∼4%) and shear strain (∼6%) [32]. The transformation at the microcrack tip tends to close the crack, and thus a portion of the energy required for fracture is spent in the stress-induced transformation. Also, the dilation in the transformed zone around a microcrack is opposed by the surrounding untransformed matrix, resulting in compressive stresses which tend to close the crack. It is therefore difficult for the microcrack to propagate, increasing the stength and toughness. Another possible explanation for the improvement in thermal shock resistance is due to the fact that during the thermal shock process, the thermal stress in the composites was relaxed, and also the matrix microcrack pinning or bridging occurred at the interface. The cracks formed at the matrix and within the SCS-9^{TM} SiC fiber by means of a thermal shock process are shown in Fig. 6.

4. Conclusion

The fracture strength of Al_2O_3 fibers/ZrO_2 composites was lower than that of monolithic ZrO_2. This is due to the high density of residual pores within the fibers and the themal stress caused by the difference in thermal expansion coefficients of the matrix and fiber. The residual pores, which were formed during fiber fabrication, acted as stress concentrators. For enhanced mechanical properties, it would be necessary to use pore-free alumina fibers. However, the addition of Al_2O_3 fibers into ZrO_2 matrix improved significantly the thermal shock resistance. This improvement may result from the pinning or bridging of matrix microcracks at the matrix/fiber interface and the relaxation of thermal stress in the composites during thermal shock process.

The addition of SiC fibers led to a significant decrease in the mechanical properties because of the formation of matrix microcracks caused by the thermal stress, but led to a significant improvement in thermal shock resistance. This improvement results from, during thermal shock process, (1) the closure of microcrack tip caused by the tetragonal-to-monoclinic phase transformation in the matrix, (2) the pinning or bridging of

matrix microcrack at the matrix/fiber interface due to the interaction between the matrix microcrack and SiC fiber, and (3) the stress relaxation in the composites.

References

1. N. CLAUSSEN, *Mater. Sci. Eng.* **71** (1985) 23.
2. K. PARK and T. VASILOS, *J. Mater. Sci.* **31** (1996) 5463.
3. *Idem., ibid.* **32** (1997) 295.
4. A. G. EVANS and D. B. MARSHALL, *Acta Metall.* **37** (1989) 2567.
5. J. W. HUTCHINSON and H. M. JENSEN, *Mech. Mater.* **9** (1990) 139.
6. A. W. HULL and E. E. BURGER, *Physics* **5** (1934) 384.
7. K. K. CHAWLA and M. METZGER, *J. Mater. Sci.* **7** (1972) 34.
8. S. MAJUMDAR, D. KUPPERMAN and J. SINGH, *J. Amer. Ceram. Soc.* **71** (1988) 858.
9. J. F. DIGREGRIO, T. E. FURTAK and J. J. PETROVIC, *J. Appl. Phys.* **71** (1992) 3524.
10. D. LEWIS and P. F. BECHER, *Ceram. Eng. Sci. Proc.* **1** (1980) 634.
11. I.-S. KIM and I.-G. KIM, *J. Mater. Sci. Lett.* **7** (1972) 34.
12. T. N. TIEGS and P. F. BECHER, *J. Amer. Ceram. Soc.* **70** (1987) C-109.
13. A. C. SOLOMAH, W. REICHERT, V. RONDINELLA, L. ESPOSITO and E. TOSCANO, *ibid.* **73** (1990) 740.
14. D. P. H. HASSELMAN, *ibid.* **53** (1970) 490.
15. T. K. GUPTA, *ibid.* **55** (1972) 249.
16. A. H. HEUER and L. H. SCHOENLEIN, *J. Mater. Sci.* **20** (1985) 3421.
17. M. ISHITSUKA, T. SATO, T. ENDO and M. SHIMADA, *J. Amer. Ceram. Soc.* **70** (1987) C-342.
18. M. ASHIZUKA, Y. KIMURA, H. FUJII, K. ABE and Y. KUBOTA, *J. Ceram. Soc. Jpn.* **94** (1986) 577.
19. W. D. KINGERY, H. K. BOWEN and D. R. UHLMANN, in "Introduction to Ceramics," edited by E. Burke, B. Chalmers and James A. Krumhansl (John Wiley & Sons, New York, 1976) p. 595.
20. A. ELKIND, M. BARSOUM and P. KANGUTKAR, *J. Amer. Ceram. Soc.* **75** (1992) 2871.
21. M. BRUN and M. BOROM, *ibid.* **72** (1989) 1993.
22. J. DICARLO, *J. Mater. Sci.* **21** (1991) 217.
23. R. W. GOETTLER and K. T. FABER, *Compos. Sci. Technol.* **37** (1989) 129.
24. J. BRIGHT, S. DANCHAIVIJIT and D. SHETTY, *J. Amer. Ceram. Soc.* **74** (1991) 114.
25. Brochure produced by Textron Specialty Materials, Lowell, MA, USA.
26. Brochure produced by Mitsui Mining Co., New York, NY, USA.
27. ASTM D790, ASTM, Philadelphia, PA, 1993.
28. K. PARK and T. VASILOS, *J. Mater. Sci. Lett.* **15** (1996) 1657.
29. J. NAKAYAMA, *Bull. Ceram. Soc. Jpn.* **8** (1973) 343.
30. R. C. GARIVE, R. H. J. HANNINK and R. T. PASCOE, *Nature (London)* **258** (1975) 703.
31. F. F. LANGE, *J. Mater. Sci.* **17** (1982) 225.
32. J. WANG and R. STEVENS, *ibid.* **24** (1989) 3421.

Received 27 July
and accepted 15 December 1998